Research Article Vol. 2, No. 3 / 15 March 2019 / OSA Continuum 629

Insights from a systematic study of crosstalk in adiabatic couplers

VINCENT NG,[1,2,3,6,*] ALESSANDRO TUNIZ,[4,5,6] JUDITH M. DAWES,[3] AND C. MARTIJN DE STERKE[4]

[1]The Dodd-Walls Centre for Photonic and Quantum Technologies, New Zealand
[2]Department of Physics, University of Auckland, Auckland 1010, New Zealand
[3]MQ Photonics Research Centre, Department of Physics and Astronomy, Macquarie University, NSW 2109, Australia
[4]Institute for Photonics and Optical Sciences (IPOS), School of Physics, University of Sydney, NSW 2006, Australia
[5]The University of Sydney Nano Institute, University of Sydney, Sydney, NSW 2006, Australia
[6]These authors contributed equally.
[*]wng299@aucklanduni.ac.nz

Abstract: We investigate how the performance of an adiabatic coupler depends on the detailed coupler properties. After verifying the accuracy of an analytic expression for the fraction of energy that is not coupled into the desired waveguide (i.e., the crosstalk), we consider how the center and the ends of adiabatic couplers contribute to the total crosstalk. We find that for short coupler lengths the center dominates, whereas for longer devices the two ends dominate.

1. Introduction

Coupling light between two waveguides is a basic and ubiquitous functionality in waveguide optics. There are broadly two classes of couplers: directional- and adiabatic- couplers. Directional couplers are formed by two neighbouring parallel waveguides, where the parameters do not depend on position [1,2]. Light at the input is coupled into a superposition of waveguide supermodes with different propagation constants, so that power transfers periodically between the individual waveguides due to modal interference. Terminating the coupler at a specific position then allows a particular fraction of the power to be transferred to the desired output waveguide; in a half-beat length coupler, for example, light completely transfers from one waveguide to the next, provided that the two supermodes have the same amplitudes. However, since the beat length depends on wavelength, directional couplers have a finite bandwidth and are thus unsuitable for some applications, e.g. nonlinear optics, which requires intense ultrashort pulses with large bandwidths.

Adiabatic couplers operate on a different principle: light is coupled into a single mode (e.g., the fundamental mode), and at least one of the waveguide parameters depends on propagation distance [3]. If the waveguide parameters evolve sufficiently slowly, then light remains in that mode, even when its nature changes completely during propagation. Adiabatic couplers enable complete power transfer between waveguides but, since the underlying mechanism does not depend on interference, their bandwidth can in principle be very large and fabrication tolerances may be relaxed. This has led to many implementations of adiabatic couplers, for both complete power transfer [4–6] and for power splitting [7]. Here, we concern ourselves with complete power transfer, where the principles of adiabatic coupling can be used, for example, for mode conversion [8,9], polarization switching [10], and efficient coupling between waveguides of vastly different optical properties and geometry [11–13].

The directional coupler is conceptually more straightforward to design: since the parameters do not vary with propagation, the amount of coupling is only determined by the ratio of the

#349141 https://doi.org/10.1364/OSAC.2.000629
Journal © 2019 Received 24 Oct 2018; revised 26 Nov 2018; accepted 11 Dec 2018; published 28 Feb 2019

OSA CONTINUUM

coupler length and the beat length of the supermodes. Adiabatic couplers are somewhat more complicated: not only do the parameters vary with propagation, but choosing the appropriate length requires balancing the incompatible needs of a small footprint (requiring a compact device) while maintaining adiabaticity (requiring a long device). In the context of integrated photonics [14,15] for example, the large footprint of adiabatic couplers (typically several hundreds of μm^2[4]) has discouraged their widespread use[5].

In this paper, we consider the case in which all the light needs to be adiabatically coupled from one waveguide to another, and, following the convention of Louisell [16], we refer to the amount of power remaining in the initial waveguide as the *crosstalk*. This analysis can broadly rely on one of two approaches. The first approach uses fully electromagnetic calculations (e.g., the Finite Element Method (FEM) and the Finite Difference Time Domain (FDTD) method) to calculate the performance of a particular device. This provides a direct result, and such calculations often form an integral part of detailed designs. However, these calculations are relatively slow, and do not provide much insight into why a particular result is obtained, or whether it can be improved (besides repeating a similar calculation on a different geometry). The second approach relies on coupled mode theory, where the coupler is described by a set of two coupled ordinary differential equations for the field amplitudes in the two waveguides. Two functions $\Delta\beta(z)$ and $\kappa(z)$ describe, respectively, the mismatch in propagation constant between the modes, and the strength of their coupling. These equations can then be efficiently solved numerically, and sometimes also analytically – at least to some approximation. Though this method is poorly suited for the final design of a particular coupler, it can provide valuable insight into how the parameters need to be changed to improve performance. In this paper we use both numerical and analytic approaches in three ways: we describe couplers through the functions $\Delta\beta(z)$ and $\kappa(z)$ to investigate performance (both numerically and analytically), and we show explicitly how these quantities relate to a physical embodiment of such adiabatic couplers through FEM calculations.

We now consider the question how to appropriately choose the profile and length of an adiabatic coupler. Much has been written on this topic, going back decades [6,8,12,13,16–22]. In a 1955 paper Louisell [16] gave a comprehensive analysis of adiabatic couplers, and provided an analytic expression for the crosstalk μ, which was based on an approximate solution to the coupled differential equations describing the system. He found that, in this approximation and for long couplers, the critical areas are the two ends of the coupler. There is a large literature on adiabatic processes in quantum mechanics with a well-known adiabaticity condition (see e.g., [23,24]), that seems to contradict the condition of Louisell: their criterion [23,24] concentrates on the region where the parameters vary fastest and the energy mismatch between the states is smallest, corresponding to the central part of a coupler. In a paper by Sun *et al.* [22], a particular family of adiabatic profiles is claimed to lead to the shortest adiabatic coupler for a given level of crosstalk μ. They exemplified their result by comparing one member of the family they identified with results from a number of other profiles. A key result of this approach is that $\mu \propto \ell^{-2}$, where ℓ is the coupler length.

Here we report a systematic study of the crosstalk of adiabatic couplers, which allows us to conclude under what conditions the center and the ends of the coupler are critical to the performance. We can also investigate the claim of Sun *et al.* [22]. While the issues raised above are conceptual, they cannot be resolved by the results reported to date, in spite of a large literature of numerical designs [8] and experiments [11]. To address the conceptual issue we consider a set of couplers in which the tapering function is given by a set of increasingly smooth polynomials $P_n(\zeta)$, where ζ varies between 0 and 1, which allow us to tailor the relative contributions of the center and the ends. This allows us to find approximate analytic expressions for all relevant parameters, and we can also vary the importance of the coupler edges and center in a systematic way. This work is based on a closed-form expression for the crosstalk provided by Louisell [16].

OSA CONTINUUM

The outline of this paper is as follows. In Section 2 we discuss the coupled mode framework that we adopt. We then evaluate the accuracy of the expression of Louisell for the crosstalk in Section 3 by comparing it with the results of a full two-dimensional COMSOL simulation and with the results of solving the coupled mode equations numerically. Then in Section 1 we conduct a systematic investigation of the effects of the ends and the center region of the coupler by using increasingly smooth taper profiles.

2. Theory

To systematically investigate the behaviour of adiabatic couplers, we start with the coupled mode equations

$$\begin{aligned} \frac{\mathrm{d}E_1}{\mathrm{d}z} &= +i\beta_1 E_1 - i\kappa E_2, \\ \frac{\mathrm{d}E_2}{\mathrm{d}z} &= -i\kappa E_1 + i\beta_2 E_2 \end{aligned} \tag{1}$$

where $E_{1,2}$ are normalized electric field amplitudes in the respective waveguides, and the power is given by $|E_{1,2}|^2$. The $\beta_{1,2}$ are the modal propagation constants and κ is the coupling strength between the waveguides. Though derived for identical waveguides, Eq. (1) can also be used to good approximation for dissimilar waveguides [25,26], provided that the waveguides are not too strongly coupled, as discussed by Snyder and Love [25]. While it is difficult to evaluate the accuracy of such an assumption *a priori*, it can be confirmed *a posteriori*, as we do here.

We define $E_{1,2} = F_{1,2}e^{i\bar{\beta}z}$, where $\bar{\beta} = (\beta_1 + \beta_2)/2$ and $\Delta\beta = (\beta_2 - \beta_1)/2$, allowing Eq. (1) to be rewritten as

$$\frac{\mathrm{d}}{\mathrm{d}z}\begin{pmatrix} F_1 \\ F_2 \end{pmatrix} = -i\begin{pmatrix} \Delta\beta & \kappa \\ \kappa & -\Delta\beta \end{pmatrix}\begin{pmatrix} F_1 \\ F_2 \end{pmatrix}. \tag{2}$$

The eigenvalues of this matrix are $\pm\Gamma$, where

$$\Gamma = \sqrt{\kappa^2 + \Delta\beta^2}. \tag{3}$$

Defining

$$\Delta\beta = \Gamma\cos\chi, \qquad \kappa = \Gamma\sin\chi, \tag{4}$$

we can write the eigenvectors of the matrix in Eq. (2) as

$$v_+ = \begin{pmatrix} -\sin\frac{\chi}{2} \\ \cos\frac{\chi}{2} \end{pmatrix}, \quad v_- = \begin{pmatrix} \cos\frac{\chi}{2} \\ \sin\frac{\chi}{2} \end{pmatrix}. \tag{5}$$

Thus, by varying χ from $0 \rightarrow \pi$ over the length of the coupler, the eigenstates evolve from one of the waveguides at the beginning of the coupler, to the other waveguide at the end of the coupler. Provided that the tuning angle χ is varied slowly enough, light remains in its original eigenstate, and thus couples from one guide to the other. In other words, light is coupled into one of the waveguides, then emerges from the other waveguide, provided that the variation is sufficiently slow. Physically, this is achieved by tuning $\Delta\beta$ through zero (i.e., from negative to positive, or vice versa) and by choosing $|\Delta\beta| \gg \kappa$ at either end of the device. The exact shapes of $\Delta\beta$ and κ are not prescribed, leading to a great variety in the possible implementations. The rate at which χ can be varied is given by the adiabaticity criterion $\eta(z) \ll 1$, where [16]

$$\eta(z) = \frac{1}{2\Gamma}\frac{\mathrm{d}\chi}{\mathrm{d}z}, \tag{6}$$

which is very similar (to within a factor of 2) to the conventional criterion for adiabaticity from quantum mechanics [23,24], and is equivalent to Eq. (5) in the paper by Sun *et al.* [22].

OSA CONTINUUM

This criterion is often used as guideline for adiabatic coupler designs, but it does not provide information on the performance of the design. Louisell [16] showed that the performance could be more directly quantified by calculating the crosstalk μ, corresponding to the optical power remaining in the initial waveguide at the end of the device, estimated via

$$\mu = \frac{1}{4}\left|\int_0^{\ell} \frac{\mathrm{d}\chi}{\mathrm{d}z'} \mathrm{e}^{-2i\rho(z')}\,\mathrm{d}z'\right|^2 = \frac{1}{4}\left|\int_0^{\rho(\ell)} \frac{\mathrm{d}\chi}{\mathrm{d}\rho'} \mathrm{e}^{-2i\rho(z')}\,\mathrm{d}\rho'\right|^2, \tag{7}$$

where ℓ is the length of the device and

$$\rho(z) = \int_0^z \Gamma(z')\,\mathrm{d}z'. \tag{8}$$

This calculated crosstalk corresponds to the square modulus of the Fourier transform of the derivative of χ with respect to Γ. When Γ is constant it corresponds to the scaled Fourier transform with respect to position. Equation (7) is based on an approximate solution to the coupled mode equations [16]. Though it is known that Eq. (7) is not accurate for short devices [16], it is not clear what "short" means in this context. In Section 3 we therefore compare the results of Eq. (3) with exact results based on coupled mode theory.

3. Verification of the expression for μ

To check the accuracy of Eq. (7), and thereby to verify that the crosstalk is given by the square modulus of the Fourier transform of the derivative of χ, we consider the particular example consisting of an adiabatic coupler consisting of two, 2-dimensional silica [27] waveguides (WGs) in air at $\lambda = 1.55\,\mu$m, shown in Fig. 1. We label the physical device length as ℓ, i.e., $0 \le z \le \ell$.

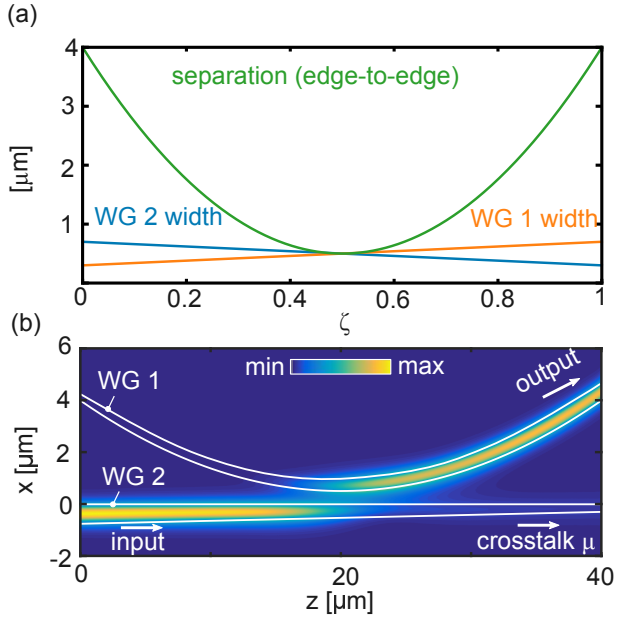

Fig. 1. Adiabatic coupler considered for calculation of the crosstalk μ. (a) Waveguide widths (blue and orange curves) and their edge-to-edge separation (green curve). The light enters in waveguide 2 and exits through waveguide 1. (b) Top view of the waveguides with Poynting vector superimposed for the particular case with $\ell = 40\,\mu$m.

OSA CONTINUUM

However, since we consider how the device performance depends on ℓ, we define a relative coordinate $\zeta = z/\ell$, so $0 \le \zeta \le 1$.

Figure 1(a) shows the width of each of the waveguides and their edge-to-edge spacing, which all depend on position. The white curves in Fig. 1(b) give an overview of the coupler. The colors show the Poynting vector for the particular example of $\ell = 40$ μm, and demonstrates that the majority of the light couples between the waveguides in the region where they approach each other most closely.

The solid curves in Fig. 2(a) show the instantaneous propagation constants (normalized to the free space wavenumber k_0) of the supermodes of the two waveguides as a function of position, whereas the dashed lines give those of the fundamental modes of the isolated waveguides. We define the instantaneous propagation constant at position ζ to be the propagation constant of a mode in an infinite, z-independent system with parameters equal to those at ζ. From the results in Fig. 2(a) we can find the coupled-mode parameters κ, $\Delta\beta$ and Γ as shown in Fig. 2(b). Note

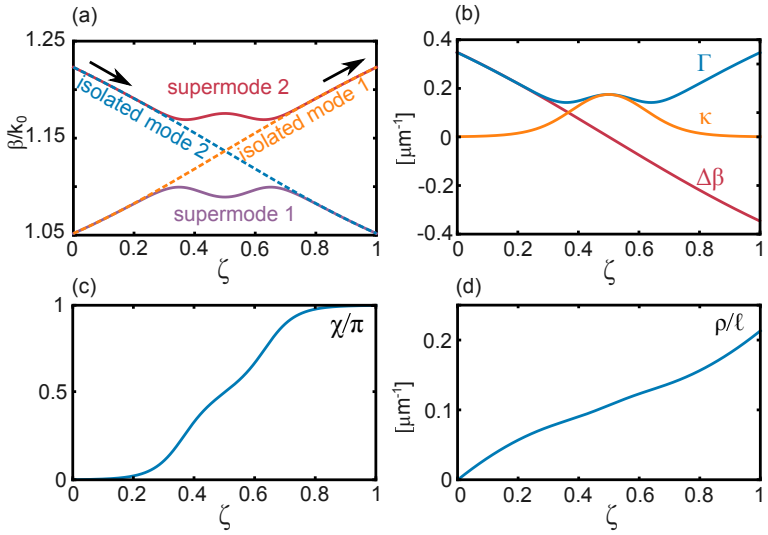

Fig. 2. Coupled-mode parameters for the adiabatic coupler shown in Fig. 1 at $\lambda = 1.55$ μm. (a) The (instantaneous) propagation of the supermodes (solid curves) and the individual waveguides (dashed). (b) Parameters $\Delta\beta$ (red), κ (orange) and Γ (blue). (c) Parameter χ. (d) Parameter ρ.

that according to Eq. (2) parameter $\Delta\beta$ corresponds to half of the difference of the dashed curves in Fig. 2(a), whereas Γ is half of the difference between the solid curves. Parameter κ can then be extracted using Eq. (3). Similarly, parameter χ can be found from Eq. (4), and is shown in Fig. 2(c). We note that, for this design, $\mathrm{d}\chi/\mathrm{d}\zeta$ is negligible at the ends and large in the center, and therefore that the center significantly impacts Eq. (6). The energy in WG 2 in this coupler, for a coupler length of 200 μm, is given in the inset of Fig. 3. The two colours refer to different methods of calculation, as discussed below.

Knowing now both the system's physical parameters as well as the coupled-mode parameters, we can calculate the crosstalk μ (or alternatively, the total power in waveguide 2 at $z = \ell$, normalized to the total intensity at $z = 0$) in three different ways. The results are summarized in Fig. 3(a) which shows μ versus device length ℓ. The blue curve gives the result of integrating Eq. (7), whereas the orange curve gives the result obtained by integrating coupled mode Eq. (2) directly. The agreement between these curves shows that Eq. (7) is accurate, at least for the parameters in this example. The largest discrepancy occurs for short lengths, where Eq. (7) is not expected to be valid [16]. Finally, the black curve gives the result of a full two-dimensional

OSA CONTINUUM

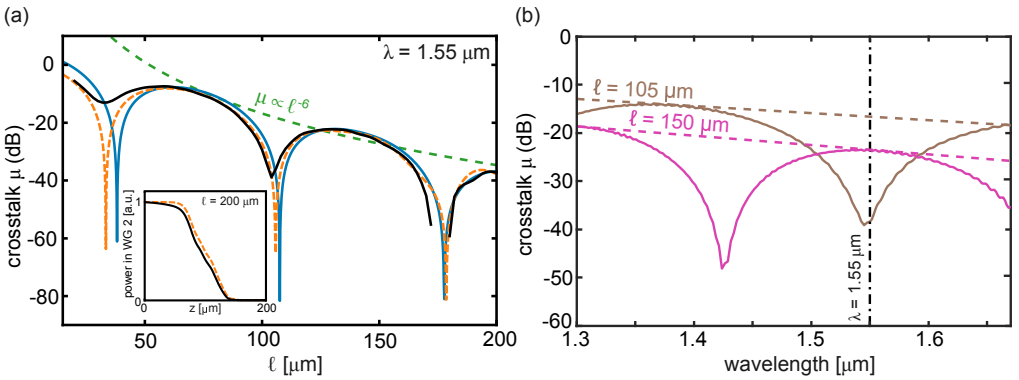

Fig. 3. (a) Crosstalk μ of the device shown in Fig. 1 as calculated using Eq. (7) (blue), integrating coupled mode Eq. (2) (orange), and using a full two-dimensional COMSOL calculation (black). Inset: power inside waveguide 1 during propagation, calculated by integrating Eq. (2) (orange), and using COMSOL (black) for $\ell = 200\,\mu$m. (b) COMSOL calculations for the crosstalk as a function of wavelength for $\ell = 105\,\mu$m (brown) and $\ell = 150\,\mu$m (purple). Dashed lines indicate the crosstalk envelope.

COMSOL calculation of the system in Fig. 1(a). Note the excellent agreement between the three curves. The only difference is that the nodes, which are quite prominent in the blue and orange curves, are somewhat less so in the black curve. This is because calculations of the small crosstalk near the nodes are susceptible to small errors. In contrast, the agreement between the overall trends is excellent, confirming the validity of Eq. (1). We note that, as expected, the crosstalk decreases with increasing device length. An analysis of Eq. (7) shows that for this example the overall trend is, approximately, $\mu \propto \ell^{-6}$.

Having established the veracity of Eq. (7), we now consider some of its consequences. Recall that the Fourier transform of a function with discontinuous m^{th} derivative, asymptotically approaches zero as the $-(m+1)$ power [28]. Since $d\chi/d\rho$ enters Eq. (7), we conclude that for sufficiently long lengths, for adiabatic couplers for which the m^{th} derivative of χ is discontinuous, the crosstalk decreases as ℓ^{-2m}. For the example considered here we find that $m = 3$ at the edges of the coupler, and thus $\mu \propto \ell^{-6}$, consistent with the numerical result in the previous paragraph. The distinctive oscillations arise from the interference between the discontinuities at $z = 0$ and at $z = \ell$. We thus conclude that, based on our expression (7) for μ, at long lengths the lowest crosstalk is achieved for couplers that are increasingly smooth at the ends. We investigate this conclusion in more detail in the next section.

The crosstalk envelope is not only amenable to analytic arguments following from Eq. (7), but it is arguably more important than the full curve itself. Since all parameters depend on wavelength, the position of the nodes in Fig. 3 is also wavelength-dependent, as shown in Fig. 3(b) for two different device lengths. In this case the envelope is therefore the relevant measure for device performance. Figure 3(b) confirms the large bandwidth of our devices: for the $\ell = 150\,\mu$m devices, the cross talk remains less than the 20 dB envelope over almost the entire wavelength range $1.3<\lambda<1.65\,\mu$m shown.

4. Coupler profiles

In this section we systematically investigate the performance of the adiabatic couplers, and in particular the effect of the coupler ends using expression (7) for μ. We do so by taking Γ to be constant and by choosing χ to be a member of the set of polynomials $\pi P_n(\zeta)$, where $P_n(0) = 0$

OSA CONTINUUM

and $P_n(1) = 1$ for all n. The $P_n(\zeta)$ are most easily defined via their first derivatives $P'_n(\zeta)$

$$P'_n(\zeta) = \frac{(2n+1)!}{(n!)^2}(\zeta(1-\zeta))^n, \tag{9}$$

so that $P_n(\zeta)$ is a $(2n+1)^{\text{th}}$-order polynomial. As an example, for $n = 2$ we find that $P'_2(\zeta) = 30\zeta^2(1-\zeta)^2$ so $P_2(\zeta) = 10\zeta^3 - 15\zeta^4 + 6\zeta^5$. It is easy to see that the $P_n(\zeta)$ has its first n derivatives equal to zero both at $\zeta = 0$ and at $\zeta = 1$. The polynomials P_0 to P_6 are illustrated in Fig. 4. It confirms that the smoothness at the edges increases with the polynomial order, but that the central region then becomes steeper. The values of the $P_n(\zeta)$ for $\zeta<0$ and $\zeta>1$ are irrelevant for our purposes here.

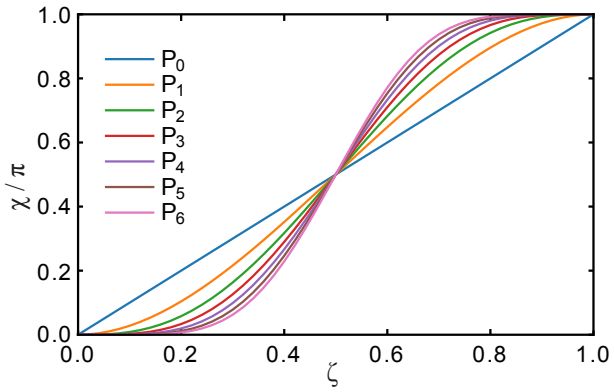

Fig. 4. Polynomials $P_n(\zeta)$ as given by Eq. (9), used to model χ.

With this choice for χ, and using Eq. (4) we can thus write

$$\begin{aligned} \kappa(z) &= \Gamma \sin(\pi P_n(\zeta)), \\ \Delta\beta(z) &= \Gamma \cos(\pi P_n(\zeta)). \end{aligned} \tag{10}$$

Figure 5 shows the crosstalk μ for $n = 1, 2, \ldots, 6$ versus the device length in units of $\ell_b = \pi/2\Gamma$, which corresponds to the device length of a directional coupler with coupling coefficient Γ. The blue curve follows from Eq. (7), whereas the orange curve follows from solving the coupled mode Eq. (2). Consistent with Section 3 these two results are very similar for low orders n, but deviate for larger n, particularly for short lengths. According to the argument in Section 3, for sufficiently large device lengths ℓ, the envelope should decrease as $\ell^{-2(n+1)}$.

For the polynomials we are using here, we can use Eq. (7) to find analytic expressions for μ. This is so because Γ is constant and the Fourier transform of any polynomial can be found in closed form. For $n = 0, 1, 2$ we find,

$$\begin{aligned} \mu_0 &= \frac{\sin(\pi\ell)^2}{4\ell^2} \\ \mu_1 &= \frac{9}{4\pi^4\ell^6}\left(-\pi\ell\cos(\pi\ell) + \sin(\pi\ell)\right)^2, \\ \mu_2 &= \frac{225}{4\pi^8\ell^{10}}\left(3\pi\ell\cos(\pi\ell) + (\pi^2\ell^2 - 3)\sin(\pi\ell)\right)^2 \\ \mu_3 &= \frac{11025}{4\pi^{12}\ell^{14}}\left(\pi\ell(\pi^2\ell^2 - 15)\cos(\pi\ell) - 3(2\pi^2\ell^2 - 5)\sin(\pi\ell)\right)^2 \end{aligned} \tag{11}$$

OSA CONTINUUM

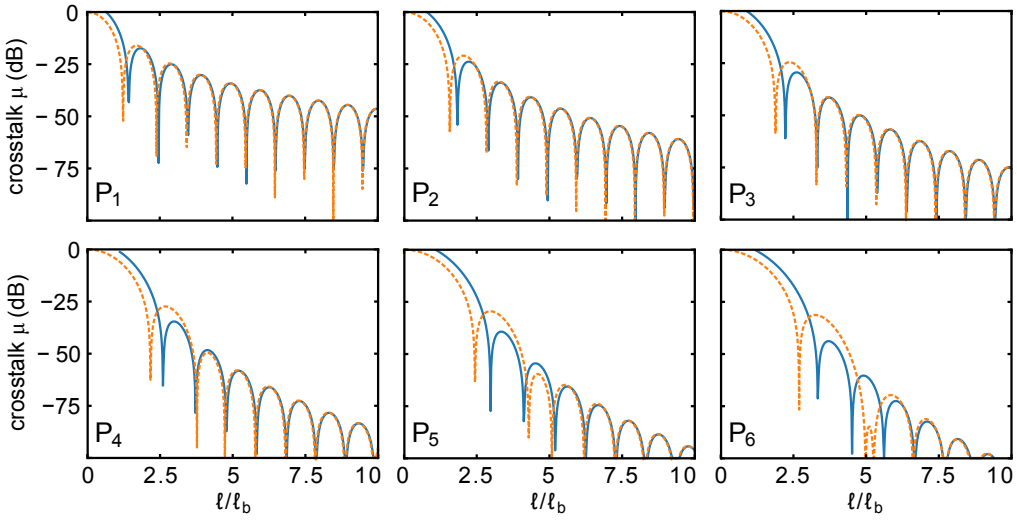

Fig. 5. Crosstalk μ versus device length, for each polynomial P_n, where $n = 1, 2, \ldots 6$, calculated by Eq. (2) numerically (blue) and from Eq. (7) (orange).

in obvious notation. We do not show results for higher order polynomials as these become increasingly complicated. We note that these are related to the squares of the spherical Bessel functions, but we do not pursue this further here.

By taking the maximum value of the oscillating terms we can find expressions for the envelope $\bar{\mu}_n(\ell)$. For $n = 0$ to 3 this leads to

$$\begin{aligned} \bar{\mu}_0 &= \left(\tfrac{1}{2\ell}\right)^2 \\ \bar{\mu}_1 &= \left(\tfrac{3}{2\pi\ell^2}\right)^2 \left(1 + \tfrac{1}{\pi^2\ell^2}\right) \\ \bar{\mu}_2 &= \left(\tfrac{15}{2\pi^2\ell^3}\right)^2 \left(1 + \tfrac{3}{\pi^2\ell^2} + \tfrac{9}{\pi^4\ell^4}\right) \\ \bar{\mu}_3 &= \left(\tfrac{105}{2\pi^3\ell^4}\right)^2 \left(1 + \tfrac{6}{\pi^2\ell^2} + \tfrac{45}{\pi^4\ell^4} + \tfrac{225}{\pi^6\ell^6}\right) \end{aligned} \tag{12}$$

with the results for higher orders more complicated but known [29]. However, it can be shown that the leading term is of the form $\bar{\mu}_n = ((2n+1)!!/(2\pi^n\ell^{(n+1)}))^2$. These results confirm the general result derived earlier that $\mu_n \propto \ell^{-2(n+1)}$ for sufficiently large ℓ. In Fig. 6 we show these envelopes for $n = 0$ to 6 (dashed lines). It shows that at increasingly long coupler lengths, the high-order couplers have the lowest crosstalk. The corresponding result obtained by solving the coupled mode Eq. (2) numerically is also shown (circles). Deviations again occur for short device lengths, though for long device lengths the results are identical.

To finish this section, we show in Fig. 7(a) the order n polynomial with the lowest crosstalk envelope versus device length. In Fig. 7(b), the blue and orange curves give the associated value of the crosstalk. These results confirm that higher order polynomials are optimal for long devices, consistent with our earlier results.

4.1. *Conventional criterion for adiabaticity*

Expression (6) is the conventional criterion for adiabaticity. Here we investigate how it is related to the analytic and numerical results for the crosstalk μ discussed in Section 4. For the particular

OSA CONTINUUM

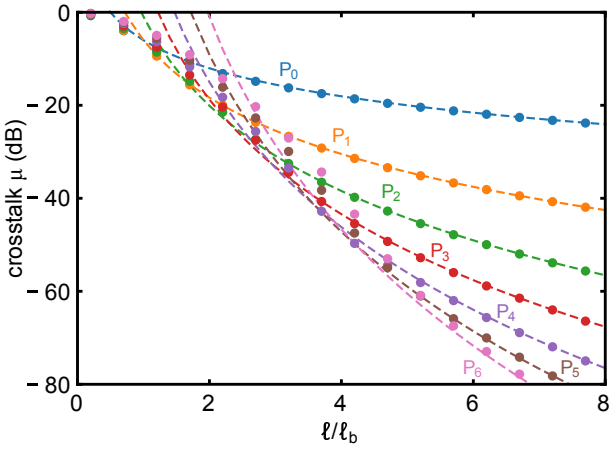

Fig. 6. Envelopes of the crosstalk μ calculated by solving couped mode Eq. (2) numerically (circles) and from Eq. (7) (dashed lines).

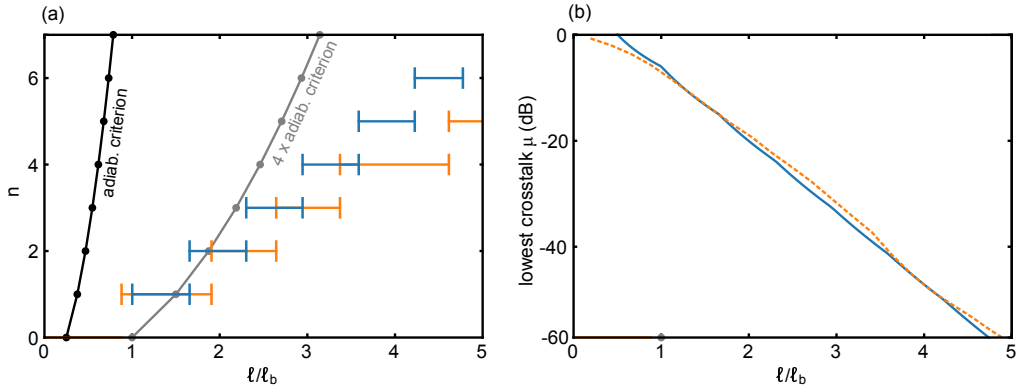

Fig. 7. (a) Black: lengths satisfying the adiabatic criterion Eq. (6) for different n, where P_n are the polynomials used for χ. Grey: 4× the length satisfied by Eq. (6). The straight horizontal lines show the range of ℓ over which polynomial order n has the lowest crosstalk, using Eq. (7) (blue) and solving Eq. (2) (orange). (b) Lowest calculated crosstalk across all polynomial orders at each length, using Eq. (7) (blue) and solving Eq. (2) (orange).

case of the polynomials (9), criterion (6) can be written as

$$\frac{\pi}{\ell} P_n'(\zeta) \ll \frac{4\pi}{\ell_b}. \tag{13}$$

Now the derivative of the polynomials peaks at $\zeta = 0.5$, where it takes the value $(2n+1)!/(n!\,2^n)^2$. Combining this with Eq. (13), then leads to

$$\frac{\ell}{\ell_b} \gg \frac{(2n+1)!}{(n!\,2^{n+1})^2}. \tag{14}$$

This result is superimposed in Fig. 7. The black dots on the left-hand side of this figure indicate the equality in this figure, whereas the gray dots indicate the equality where the left-hand side is four times as large as the right-hand side.

In discussing these results we note that result (7) highlights the ends of the coupler, at least for long couplers, whereas inequality (14), which is derived from it, only depends on the properties

OSA CONTINUUM

of the tapered region in the center. These seemingly contradictory results arise since the argument leading to coupler ends being crucial is an asymptotic argument. Indeed, we find that for moderate value of the crosstalk (i.e., $\mu \gtrsim 10^{-4}$), criterion (14) is more relevant, whereas for lower values of the crosstalk, $\mu \lesssim 10^{-6}$, the asymptotic analysis is more appropriate.

5. Discussion and conclusions

We have demonstrated that the crosstalk μ accurately predicts the performance of adiabatic couplers, with a strong agreement between the analytic, numeric and simulation methods presented here, particularly for long designs. This form of the crosstalk is useful in providing insights into general features of adiabatic couplers, such as the emergence of oscillations as a function of length. We have also considered the crosstalk of adiabatic couplers using a systematic approach that relies on the use of increasingly smooth polynomials to describe the taper function. Using these polynomials, it is possible to find analytic expressions for many of the relevant criteria for the performance of the adiabatic coupler, including the crosstalk.

The evaluation of different criteria for adiabaticity can be confusing since some authors emphasize the center of the coupler, where the coupler properties tend to vary most rapidly, whereas other authors emphasize the ends, where the coupler properties inevitably exhibit discontinuities. We find that both affect the performance of the design, with the former more relevant for relatively short couplers with modest values for the crosstalk, and the latter more relevant to longer couplers for which the crosstalk is much lower. Which of these criteria is most relevant in a particular situation depends on the crosstalk that is required, which, in part, depends on the fabrication quality that can be achieved. However, as a rough guide, Fig. 6 shows that the device's ends determine the cross coupling for $\ell \gg \ell_b$, whereas the center limits the device's performance for $\ell \lesssim \ell_b$

We are now also in a position to evaluate the claim of Sun *et al.* [22]: that theirs is the shortest coupler for a given value of the crosstalk. In fact, they propose a family of couplers with this property, one member of which is considered in detail in the paper [22]. It can be shown that another member of this family is also one of the polynomials considered in Section 4, namely $P_0(\zeta)$. As discussed, the crosstalk for couplers following this polynomial scales as ℓ^{-2}. We saw in Section 4 that couplers following higher-order polynomials scale in a superior way with length, and therefore a coupler that follows a polynomial of higher order performs better at sufficiently long coupler lengths.

We note that we have not considered the couplers that follow from adiabatic invariants and the introduction of counterdiabatic terms [30–32], and which can have reduced cross talk in short devices. We will consider these types of approaches in future publications.

In conclusion, we have conducted a systematic study of the crosstalk in adiabatic couplers and reconciled two seemingly contradictory adiabaticity criteria. We find that the central coupler region determines the crosstalk for short devices, whereas for longer devices the crosstalk is determined by the smoothness of the coupler ends. Though we have considered only a single set of functions for which analytic results can be obtained, our conclusions are general and apply to a broad set of couplers.

Funding

University of Sydney.

Acknowledgments

A. T. acknowledges funding from the University of Sydney Postdoctoral Fellowship scheme.

OSA CONTINUUM

References

1. E. A. Marcatili, "Dielectric rectangular waveguide and directional coupler for integrated optics," Bell Syst. Tech. J. **48**(7), 2071–2102 (1969).
2. D. Marcuse, "The coupling of degenerate modes in two parallel dielectric waveguides," Bell Syst. Tech. J. **50**(6), 1791–1816 (1971).
3. J. S. Cook, "Tapered velocity couplers," Bell Syst. Tech. J. **34**(4), 807–822 (1955).
4. Z. Lu, H. Yun, Y. Wang, Z. Chen, F. Zhang, N. A. Jaeger, and L. Chrostowski, "Broadband silicon photonic directional coupler using asymmetric-waveguide based phase control," Opt. Express **23**(3), 3795–3808 (2015).
5. K. Solehmainen, M. Kapulainen, M. Harjanne, and T. Aalto, "Adiabatic and multimode interference couplers on silicon-on-insulator," IEEE Photonics Technol. Lett. **18**(21), 2287–2289 (2006).
6. H. Oukraou, L. Vittadello, V. Coda, C. Ciret, M. Alonzo, A. A. Rangelov, N. V. Vitanov, and G. Montemezzani, "Control of adiabatic light transfer in coupled waveguides with longitudinally varying detuning," Phys. Rev. A **95**(2), 023811 (2017).
7. J. Xing, Z. Li, X. Xiao, J. Yu, and Y. Yu, "Two-mode multiplexer and demultiplexer based on adiabatic couplers," Opt. Lett. **38**(17), 3468 (2013).
8. N. Riesen and J. D. Love, "Ultra-broadband tapered mode-selective couplers for few-mode optical fiber networks," IEEE Photonics Technol. Lett. **25**(24), 2501–2504 (2013).
9. D. Dai and M. Mao, "Mode converter based on an inverse taper for multimode silicon nanophotonic integrated circuits," Opt. Express **23**(22), 28376 (2015).
10. C. Sun, Y. Yu, G. Chen, and X. Zhang, "A Low Crosstalk and Broadband Polarization Rotator and Splitter Based on Adiabatic Couplers," IEEE Photon. Technol. Lett. **28**(20), 2253–2256 (2016).
11. S. Gröblacher, J. T. Hill, A. H. Safavi-Naeini, J. Chan, and O. Painter, "Highly efficient coupling from an optical fiber to a nanoscale silicon optomechanical cavity," Appl. Phys. Lett. **103**(18), 181104 (2013).
12. J. Mu, M. Dijkstra, Y.-S. Yong, F. B. Segerink, K. Wörhoff, M. Hoekman, A. Leinse, and S. M. García-Blanco, "Low-loss, broadband and high fabrication tolerant vertically tapered optical couplers for monolithic integration of Si_3N_4 and polymer waveguides," Opt. Lett. **42**(19), 3812–3815 (2017).
13. R. S. Daveau, K. C. Balram, T. Pregnolato, J. Liu, E. H. Lee, J. D. Song, V. Verma, R. Mirin, S. W. Nam, L. Midolo, S. Stobbe, K. Srinivasan, and P. Lodahl, "Efficient fiber-coupled single-photon source based on quantum dots in a photonic-crystal waveguide," Optica **4**(2), 178–184 (2017).
14. L. Chrostowski and M. Hochberg, *Silicon Photonics Design: From Devices to Systems* (Cambridge University Press, 2015).
15. L. Thylén and L. Wosinski, "Integrated photonics in the 21st century," Photon. Res. **2**(2), 75–81 (2014).
16. W. H. Louisell, "Analysis of the single tapered mode coupler," Bell Syst. Tech. J. **34**(4), 853–870 (1955).
17. H. Yajima, "Dielectric thin-film optical branching waveguide," Appl. Phys. Lett. **22**(12), 647–649 (1973).
18. R. B. Smith, "Analytic solutions for linearly tapered directional couplers," J. Opt. Soc. Am. **66**(9), 882–892 (1976).
19. Y. Silberberg, P. Perlmutter, and J. Baran, "Digital optical switch," Appl. Phys. Lett. **51**(16), 1230–1232 (1987).
20. T. A. Ramadan, R. Scarmozzino, and R. M. Osgood, "Adiabatic couplers: Design rules and optimization," J. Lightwave Technol. **16**(2), 277–283 (1998).
21. S. Longhi, G. Della Valle, M. Ornigotti, and P. Laporta, "Coherent tunneling by adiabatic passage in an optical waveguide system," Phys. Rev. B **76**(20), 201101 (2007).
22. X. Sun, H.-C. Liu, and A. Yariv, "Adiabaticity criterion and the shortest adiabatic mode transformer in a coupled-waveguide system," Opt. Lett. **34**(3), 280–282 (2009).
23. L. I. Schiff, *Quantum Mechanics*, 2nd ed. (McGraw-Hill, 1955).
24. N. V. Vitanov, T. Halfmann, B. W. Shore, and K. Bergmann, "Laser-induced population transfer by adiabatic passage techniques," Annu. Rev. Phys. Chem. **52**(1), 763–809 (2001).
25. A. W. Snyder and J. D. Love, *Optical Waveguide Theory* (Chapman and Hall, 1983), chap. 29.
26. D. Marcuse, "Directional couplers made of nonidentical asymmetric slabs. part i: Synchronous couplers," J. Lightwave Technol. **5**(1), 113–118 (1987).
27. I. H. Malitson, "Interspecimen comparison of the refractive index of fused silica," J. Opt. Soc. Am. **55**(10), 1205–1209 (1965).
28. R. N. Bracewell, *The Fourier Transform and its Applications*, 2nd ed (McGraw-Hill, 1983).
29. F. W. J. Olver and L. C. Maximon, "Bessel functions", in *NIST Handbook of Mathematical Functions*, F. W. J. Olver, D. W. Lozier, R. F. Boisvert, and C. Clark, eds. (Cambridge University Press, 2010).
30. M. Demirplak and S. A. Rice, "Adiabatic population transfer with control fields," J. Phys. Chem. A **107**(46), 9937–9945 (2003).
31. C.-P. Ho and S.-Y. Tseng, "Optimization of adiabaticity in coupled-waveguide devices using shortcuts to adiabaticity," Opt. Lett. **40**(21), 4831–4834 (2015).
32. S. Martínez-Garaot, J. G. Muga, and S.-Y. Tseng, "Shortcuts to adiabaticity in optical waveguides using fast quasiadiabatic dynamics," Opt. Express **25**(1), 159–167 (2017).